SHEAR CAPACITY OF RC BEAMS CONTAINING CORRODED LONGITUDINAL BARS

X. XUE[1*†], H. SEKI[2], and Z. W. CHEN[3]

[1] *School of Architecture and Civil Engineering, Xiamen University, China*
[2] *Department of Civil and Environmental Engineering, School of creative Science and Engineering, Waseda University, Japan*
[3] *School of Architecture and Civil Engineering, Xiamen University, China*

ABSTRACT

The effect of corroded longitudinal bars on shear behavior of RC beams containing stirrups was experimentally investigated. Based on experimental results, it was found that, as longitudinal bar corrodes, deterioration in bond effect due to corrosion causes a transformation of load-carrying mechanism and thus results in the increase in shear capacity of RC beams. Assuming that the support points in corroded specimens shift toward the loading position, the shear capacity can be predicted accurately basing on "modified truss analogy".

Keywords: Corrosion, Longitudinal bars, Shear capacity, Load-carrying mechanism, Shear span.

1. INTRODUCTION

For RC members subjected to chloride-attack action or concrete carbonation, steel bar corrosion is one of the most critical subsequences, which can impair the structural performance (JSCE 2006; Hong 2006). For a RC beam containing corroded steel bars, the flexural performance has been widely investigated (Azad et al. 2010; Wang and Chen 2011; Jin et al. 2009; Hayashi et al. 2009). However, for the shear performance, the shear behavior of corroded RC beams is very complicated, the deterioration mechanism of shear performance has yet to be made clear. Since shear failure of RC members is relatively brittle and can occur without sufficient warning, the shear performance of corroded RC beams should be paid more attention.

In a RC beam, once longitudinal bars corrode, the following subsequences occur: sectional area loss of steel bars, generation of corrosion cracks in concrete, and deterioration in bond strength between steel bars and the surrounding concrete. The sectional area loss of longitudinal bars is generally thought to have little influence on the shear behavior; regarding the corrosion cracks, since the cracks impair the integrity of tensile zone concrete, the stiffness of RC beams will decrease (JSCE 2006); the influence of the deterioration in bond strength due to corrosion has been paid more

* Corresponding author: Email: xuexin@xmu.edu.cn

† Presenter: Email: xuexin@xmu.edu.cn

attention by published literatures. Numerous researches (Sato et al. 2003; Matsuo et al. 2004; Hashimoto et al. 2003; Xue et al. 2009) have pointed out that, when longitudinal bars corrode, tie-arch mechanism strengthen, truss mechanism weaken, which is termed “load-carrying mechanism transfer” in this paper. However, to what extent the load-carrying mechanism will change, and how much the shear capacity is, has not been made clear. Therefore, there is a need to develop a method that can quantitatively predict the shear capacity of RC beams containing corroded longitudinal bars.

Given the above mentioned background, this research carried out an experimental investigation on the effect of longitudinal bar corrosion on shear behavior of RC beams and made an attempt to develop a proper method that can reasonably predict the shear strength of RC beams containing corroded longitudinal bars.

2. EXPERIMENTAL DETAILS

2.1. Details of specimens

Specimen details are shown in Figure 1. The specimen sections were designed as 12cm in width and 24cm in height. To avoid flexural failure, high strength screw-type steel bars were used for the longitudinal bars. Round bars φ6 were used for the stirrups with close-type. Spacing of stirrups was designed as 120mm, equivalent to 0.39% of steel ratio. Mechanical properties of the reinforced steel bars are shown in Table 2. To avoid premature anchorage failure due to steel bar corrosion, the two ends of the longitudinal bars were fixed to the steel plates placed outside the specimens using nut. Since only the longitudinal bas were subjected to accelerated corrosion tests (will be described later), insulating job was done to the contact area between the longitudinal bars and the stirrups to prevent stirrup corrosion.

Experimental details are shown in Table 1. Experimental parameters were longitudinal bar corrosion levels and shear span to effective depth ratio (*a/d*). The specimens can be divided into three series with different *a/d*, and each series contained one sound specimen and two corroded specimens. The mix proportion of concrete is specified in Table 3. The specimens had been moist cured for one week and then dry cured for at least 28 days since concrete placement. Loading test was carried out soon after the accelerated corrosion test. 28 day compressive strength of each specimen is also specified in Table 1.

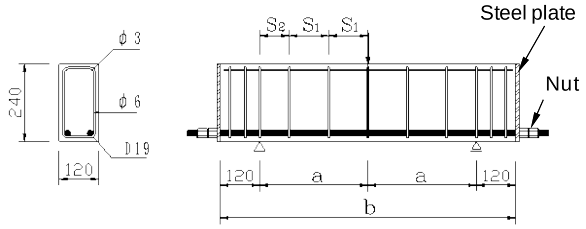

Series	*a* (mm)	*b* (mm)	*a/d*	S_1 (mm)	S_2 (mm)
B(2.0)-ms	440	1120	2.0	120	80
B(2.6)-ms	580	1400	2.6	120	100
B(3.2)-ms	700	1640	3.2	120	100

Figure 1: Details of specimens.

Table 1: Experimental details and test results

Specimens[1)]	a/d	f_c' [2)] (N/mm²)	Mass loss(%)		V_u [3)] (kN)	Virtual		a'/d	$V_{u\text{-}val}$ [4)] (kN)	$V_{u\text{-}val}/V_u$
			PAM	*PMM*		a´(mm)	a´/a			
B(1.5)-ms	1.5	36.0	0.0	0.0	108.3	--	--	1.5	108.3	1.00
B(1.5)-m1s		36.0	6.4	12.0	124.3	310	0.94	1.4	113.2	0.91
B(1.5)-m2s		37.0	9.6	16.6	115.0	310	0.94	1.4	113.4	0.99
B(2.0)-ms	2.0	38.0	0.0	0.0	81.9	--	--	2.0	81.9	1.00
B(2.0)-m1s		39.1	7.8	15.1	89.3	380	0.86	1.7	95.2	1.07
B(2.0)-m2s		39.3	9.1	15.0	103.1	330	0.75	1.5	109.1	1.06
B(2.6)-ms	2.6	33.1	0.0	0.0	74.0	--	--	2.6	74.0	1.00
B(2.6)-m1s		35.1	3.1	5.0	77.4	470	0.81	2.1	76.6	0.99
B(2.6)-m2s		35.9	18.4	32.0	82.1	430	0.74	2.0	93.9	1.14
B(3.2)-ms	3.2	35.2	0.0	0.0	70.6	--	--	3.2	70.6	1.00
B(3.2)-m1s		34.9	5.0	8.0	70.5	680	0.97	3.1	69.8	0.99
B(3.2)-m2s		33.3	6.0	8.5	71.7	675	0.96	3.1	70.5	0.98

1) B(2.6)-m×s: ms: no corrosion, sound specimens; m1s: longitudinal bar corrosion level = level 1

2) f_c' : Compressive strength of concrete, 3) V_u: shear strength (test results)

4) $V_{u\text{-}eval}$: shear strength (evaluation results)

Table 2: Steel bar properties

Steel bars	Specification		Sectional area (mm²)	Yield strength (N/mm²)
Longitudinal	D19	USD685	287	706
Stirrups	ø6	SR235	28	300

Table 3: Mix proportion

W/C (%)	s/a (%)	Unit(kg/m3)				
		Cement	Water	Fine aggregate	Coarse aggregate	Admixture
48.1	51.8	387	186	881	842	5.8

2.2. Accelerated corrosion test

Electrochemical corrosion tests shown in Figure 2 were carried out to accelerate steel bar corrosion in a short period. The specimens were immersed in 3% NaCl solution for about 24 hours, and then the longitudinal bars and a copper plate placed outside the specimen were connected to the anode and cathode of a constant current generator respectively. The amount time of the corrosion test was controlled to achieve different corrosion levels.

After loading tests, the specimens were demolished and the steel bars were taken out for corrosion state investigation. The concrete debris and some corrosion products were firstly roughly removed using a sand blast, and then the corroded steel bars were put in 10% ammonium hydrogen citrate solution for 24 hours to achieve a thorough cleaning.

Two indexes of *PAM* (percentage average mass loss) and *PMM* (percentage maximum local mass loss) were used to evaluate average corrosion state and local severe corrosion state respectively. The *PAM* of the steel bars can be calculated using equation (1).

$$PAM = \Delta w / w \times 100 \quad (1)$$

Where Δw is the average mass loss of corroded stirrups, and w is the mass of original stirrups.

The *PMM* of longitudinal bars was acquired by comparing the minimum residual sectional area visually detected and the original sectional area. The minimum residual sectional area could be measured using a caliper, and calculated by assuming it as ellipse shape.

The specimens were subjected to loading tests under simply supported conditions, as shown in Figure 3. The load was applied at mid span with a displacement increment of 0.2 mm/minute. Application of the load was monitored using load cell, and the deflection was measured using linear variable differential transformers displacement transducers (LVDT) placed beneath the soffit of specimens at the loading position. During the loading test, the opening of critical inclined cracks, which result in the ultimate failure of beams, was also measured using a visual crack comparator.

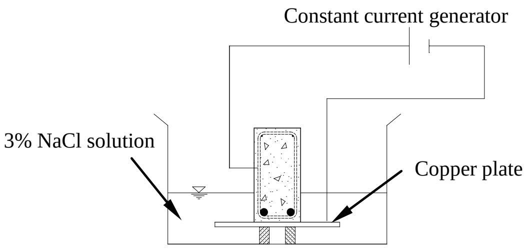

Figure 2: Accelerated corrosion test

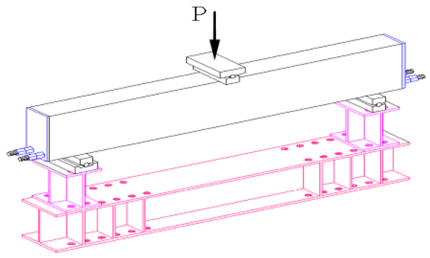

Figure 3: Loading test

3. RESULTS AND DISCUSSION

3.1. Corrosion state of longitudinal bars

For all the specimens subjected to accelerated corrosion tests, rust stains and cracks along the longitudinal bars were confirmed along the longitudinal bars on the concrete surface. These cracks are thought to be caused by the expansion of corrosion products.

3.2. Loading test results and discussion

The relationship between shear strength V_u and *PAM* is shown in Figure 4, indicating that all the corroded specimens show higher shear strength than that of the sound specimens, and for the same *PAM*, shear strength exhibited less increase in shear strength as *a/d* increased.

The critical inclined crack opening behavior of B(2.6)-ms series is shown in Figure 5. It can be observed that the opening of the critical inclined crack slowed down with the increase of the corrosion level of longitudinal bars. The same intendancy is confirmed in B(2.0)-ms and B(3.2)-ms series. Because the narrower the inclined crack, the more significant the interlock shear transfer effect, it can be expected that the shearing force carried by interlock shear transfer increased with the corrosion level of longitudinal bars.

The crack patterns at failure are shown in Figure 6. Compared with the sound specimens, the number of flexural cracks in corroded specimens decreased and the critical inclined crack shifted gradually to the loading position and kept the same inclination approximately equaling to 45 degree to the axial direction. As a result, the area of compression zone of concrete above the end of the critical inclined crack became larger than that of the sound specimens, and therefore the shearing force carried by compression zone concrete increased. On the other hand, since the projection of the critical inclined crack on axial direction became shorter, the number of the stirrups intersecting the critical inclined crack decreased, and therefore the shearing force carried by stirrups.

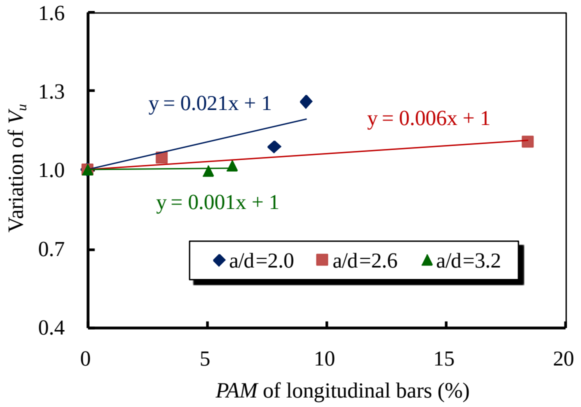

Figure 4: V_c - *PAM* relationships

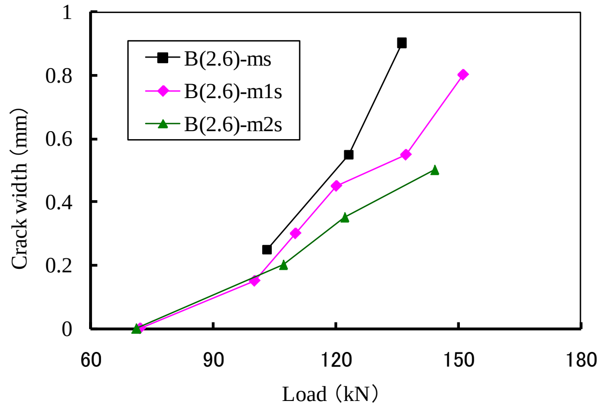

Figure 5: Crack width behavior (B(2.6)-ms series)

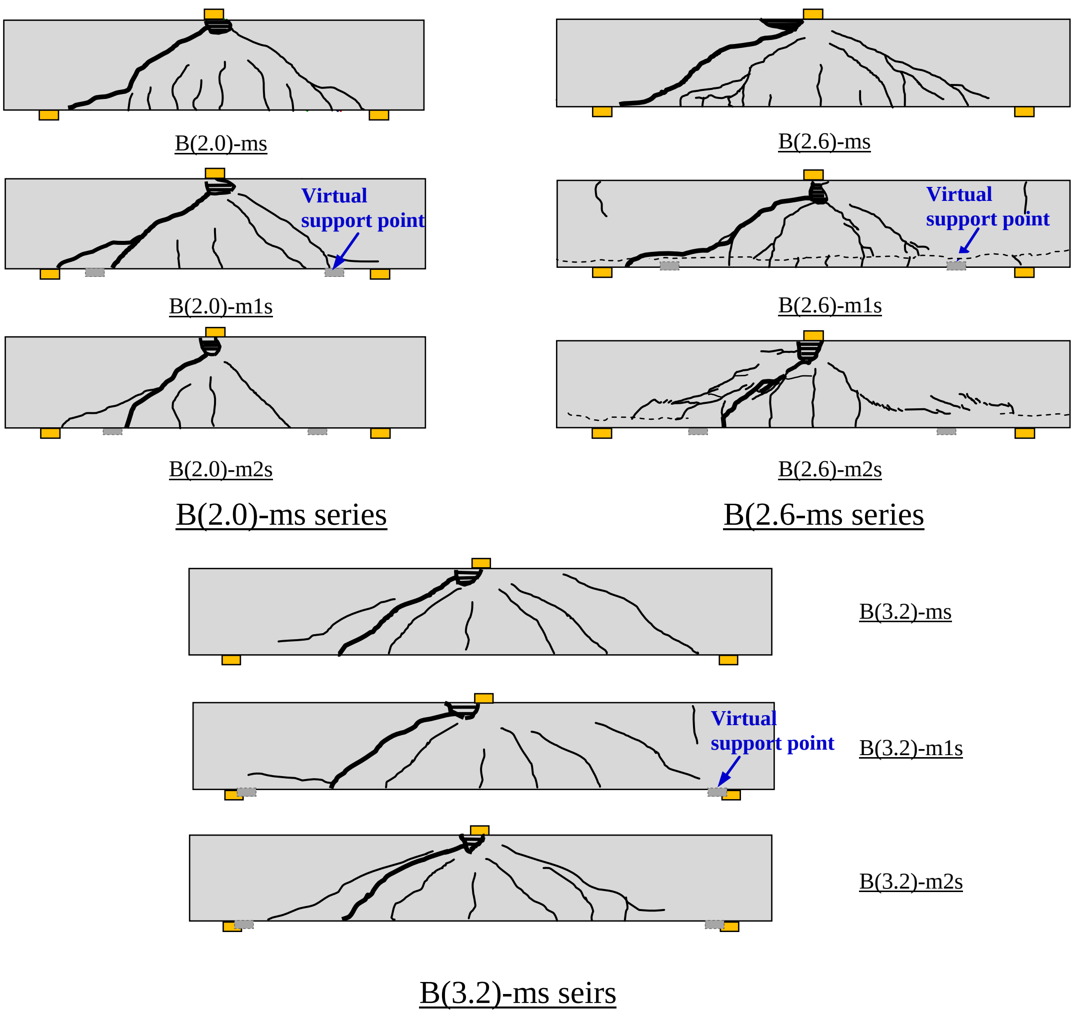

Figure 6 Crack patterns at failure

Since the shearing force carried by compression zone concrete and interlocks shear transfer effect in corroded specimens increased, whereas the shearing force carried by stirrups decreased, it is reasonable to expect that tie-arch mechanism in corroded specimens strengthened, truss mechanism weakened, which means that the corrosion of longitudinal bars caused a transfer of load-carrying mechanism. In the corroded specimens, the role of stirrups placed near the support was to prevent the propagation of bond crack and enhance flexural rigidity of longitudinal bars, and thus made the tie-arch mechanism stronger.

As the longitudinal bar corroded, the critical inclined crack shifted to the loading position, which is similar to the crack behavior of specimens with small *a/d*. Therefore, it is naturally to speculate that the shear strength of specimens containing corroded longitudinal bars can be evaluated reasonably using “modified truss analogy” by assuming that the support point shifts toward the loading position. In this paper, the shifted support point is termed “virtual support point”. The position of virtual support point was determined from the shifting distance of the critical inclined crack on axial direction and marked in figure 6. The distance from the virtual support point to the loading point is defined as virtual shear span a´ and specified in table 1.

The changing ratio of *a´/a* was calculated and plotted to the *PAM* in Figure 7, good correlation is confirmed in between, *a´/a* decreased approximately linearly with the increase of *PAM* of longitudinal bars.

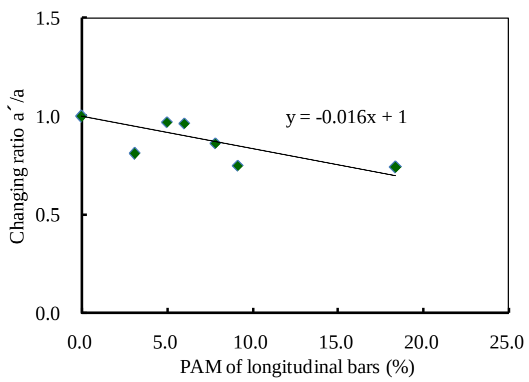

Figure 7: *a´/a-PAM* relationships

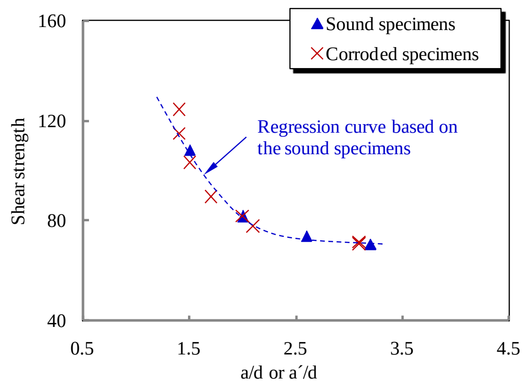

Figure 8: V_u – *a/d* or *a´/d* relationship

Figure 8 shows the relationship between shear strength and *a/d* (sound specimens) or *a´/d* (corroded specimens). Regression curve based on the sound specimen results is drawn in dot line. It can be observed that the shear strength decreased with the increase of *a/d*, which reflecting the effect of shear span. It can be confirmed that the results of corroded specimens with various *a´/d* scatters near the regression line. It implies that using virtual shear span *a´*, the shear strength can be predicted reasonably using traditional shear theory, just as the sound specimens.

In accordance with “modified truss analogy”, which is widely used to evaluate shear strength of RC beams in many countries’ building code, shear strength $V_{u\text{-}eval}$ equals to V_c carried by concrete through tie-arch mechanism plus V_s carried by stirrups through truss mechanism (Fenwick and Paulay 1968), as shown in equation (2).

$$V_{u-val} = V_c + V_s \tag{2}$$

V_s can be calculated in accordance with "truss analogy" as shown in equation (3).

$$V_s = f_y \cdot A_w \cdot \cdot jd / S \tag{3}$$

Where f_y is yield strength of stirrups, A_w is cross-sectional area of stirrups, j is a coefficient generally taken as 1/1.15, d is the effective depth of beams, S is the spacing of stirrup.

V_c equals to the shear strength of corresponding RC beams without stirrups. and can be calculated using equation (4) or equation (5), V_c=Max(V_{c1},V_{c2}). (Tanabe et al. 2000)

For diagonal tension failure of the corresponding beams without stirrups (Niwa et al. 1986):

$$V_{c1} = 0.2 f_c'^{1/3} (100 p_t)^{1/3} \left(\frac{10^3}{d}\right)^{1/4} \left(0.75 + \frac{1.4d}{a}\right) b_w d \tag{4}$$

For shear compression failure of corresponding beams without stirrups (Niwa 1983):

$$V_{c2} = \frac{0.24 f_c'^{2/3} (1 + \sqrt{100 p_t})(1 + 3.33 r / d)}{1 + (a/d)^2} b_w d \tag{5}$$

Evaluation results of shear strength are shown in Table 1. Figure 8 shows relationship between $V_{u\text{-}eval}/V_u$ and *PAM* of longitudinal bars. It can be observed that the evaluation results match well with the text results.

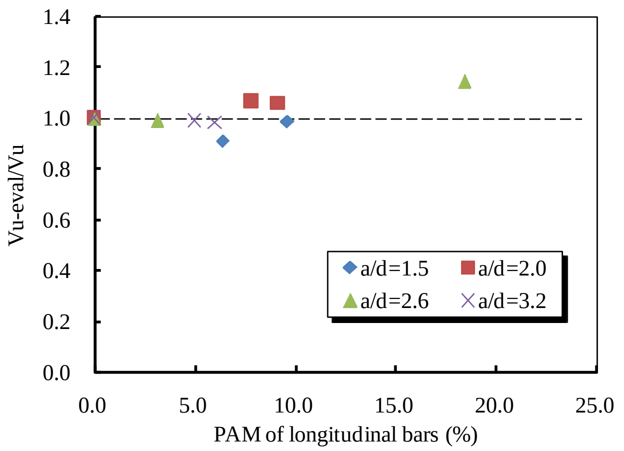

Figure 9: Relationship between V_u-*eval*/V_u and *PAM* of longitudinal bars

4. CONCLUSIONS

The shear behavior of RC beams containing corroded longitudinal bars was investigated, and with the scope of this paper, the following conclusions can be drawn:

1) Longitudinal bar corrosion might cause load-carrying mechanism transfer. The deterioration in bond strength of longitudinal bars resulted in the enhancement of tie-arch mechanism, and thus increased the shear strength of RC beams.

2) The transfer of load-carrying mechanism due to longitudinal bar corrosion was affected by the shear span to effective depth ratio (*a/d*) of RC beams. As *a/d* became larger, the transfer of load-carrying mechanism became less significant.

3) Making an assumption that the support point shifted gradually toward the loading position, the shear strength of RC beams containing corroded longitudinal bars could be evaluated accurately using the traditional “modified truss analogy”.

REFERENCES

Azad AK, Ahmad S, and Al-Gohi BHA (2010). flexural strength of corroded reinforced concrete beams. Magazine of Concrete Research. 62(6). pp. 405-414.

Fenwick RC and Paulay T (1968). Mechanisms of shear resistance of concrete beams. Journal of the Structural Division ASCE. 94(ST10). pp. 2235-2350.

Hashimoto K, Morigawa H, and Kabayashi H (2003). Evaluation on shear behavior of reinforced concrete beams containing corroded steel bars. Proceeding of Japan Concrete Institute. 25(2). pp. 1009-1014.

Hong H (2006). Architectural Corrosion and Sustainable Development. Industrial Construction. 36(3). Pp. 76-79.

Hayashi K, Tsubaki K, and Hosoda A (2009). Influence of internal structure of flexural crack on steel corrosion of reinforced concrete members. Doboku Gakkai Ronbunshuu). 65(4). pp. 577-588.

JSCE (2006). Concrete technology series, No.71: Structural performance of concrete structure containing deteriorated materials, Japan Society of Civil Engeers, Tokyo, Japan.

Jin WL, Xia j, Jiang AY, and Wang HL (2009). Flexural capacity of corrosion-damaged RC beams. China Civil Engineering Journal. 42(11). pp.64-70.

Matsuo T, Sakai L, Matumura T, and Kanetsu T (2004). Studies on the shear load carrying mechanism of RC beams with corroded reinforcement. Concrere Journal. 15(2). pp. 69-77.

Niwa J (1983). Shear equation of deep beams based on analysis. Proceedings of JCI 2nd colloquium on shear analysis of RC structures, Tokyo, pp. 119-128.

Niwa J, Yamata H, Yokozawa W, and Okamura H (1986). Revaluation of the equation for shear strength of reinforced concrete beams without web reinforcement. Journal of Materials, Concrete Structures and Pavement. 372. pp. 167-176.

Sato Y, Yamamoto T, and Hattori A (2003). Influence of shear behavior of RC members containing longitudinal bars and stirrups. Proceedings of the Japan Concrete Institute. 25(1). pp. 821-826.

Tanabe,T, Higai, T, Umehara, H, and Niwa, J (2000). Concrete Structure. Asakura Publishing Co., Ltd. Second Edition.

Wang Wl and Chen J (2011). Residual strengths of reinforced concrete beams with heavy deterioration. Research Journal of Applied Sciences. Engineering and Technology. 3(8). pp. 798-805.

Xue X, Hiromori S, and Seki H (2008). Influences of shear-span ratio on the shear behavior of RC beams due to reinforcing bar corrosion. Proceedings of the Japan Concrete Institute. 30(3). pp. 745-750.

Xue X, Seki H and Hiromori S (2009). Influence of reinforceing bar corrosion on shear behavior of RC beams. Doboku Gakkai Ronbunshuu E. 65(2). pp. 161-177.